Particle Physics Laboratory Class

Experiment T13 | Paul Trap

Jonas Lieb (312136)
Jöran Stettner (312169)

RWTH Aachen

April 3, 2017

Contents

Chapter 1

Introduction and Theory

In this laboratory report, the storage of charged particles and a measurement of their specific charge is presented. The experiment consists of a Paul trap, named after its creator Wolfgang Paul, which constrains the movement of ionized aluminum powder particles to stable trajectories by applying three alternating electrical fields.

1.1 Trapping Particles in Electrical Fields

Beside the storage of charged particles by B-fields, it is possible to trap particles in electrical fields. In a static electrical field of arbitrary shape, the particle will follow the field lines and finally hit the source of the field (e.g. the capacitor plate) or diverge (e.g. field of charged sphere). However, with time dependent fields it is possible to create an electrical potential which has a minimum when averaged over time. If the period of these fields is smaller than the typical timespan of the particles' movement inside the trap, a stable trajectory exists and the particle gets trapped.

In this setup, the magnetic fields created by changing electric fields can be neglected. This is due to the factor of $1/c^2$ in the Maxwell equation $\boldsymbol{\nabla} \times \vec{\mathbf{B}} = \frac{1}{c^2} \frac{\partial \vec{\mathbf{E}}}{\partial t}$.

In a cubic geometry (6 plates, opposing plates at same potential), the following equation of motion holds for all three dimensions. In this so called Mathieu equation, the index i stands for the three spatial components, Ω is the frequency of the alternating fields, $\xi = \frac{1}{2}\Omega t$ is the normalized time and a_i, q_i are constants depending on the applied voltages and the particle's properties.

$$\left(a_i + q_i \cos(2\xi)\right) x_i + \frac{d^2 x_i}{d\xi^2} = 0 \tag{1.1}$$

The full solution of this equation is discussed elsewhere (e.g. in the lab manual[1]), only the following aspects are important for the conducted experiment.

1.1.1 Stability of the Particle Trajectories

The exact solution for the particle trajectories can be expressed as an infinite series. However, the tracks are only finite under certain conditions. Depending on the applied alternating field U_i and the constant field U' (same potential on both plates), the constants a and q change. The constants in x-direction are given in equation 1.2 and 1.3, where K

is a geometry factor of the plates, m the mass of the particle, q the charge of the particle and r_0 the distance of the plates to the center.

$$a_x = \frac{16Kq}{3\Omega^2 m r_0^2} U' \tag{1.2}$$

$$q_x = \frac{-4Kq}{\Omega^2 m r_0^2} U_x \tag{1.3}$$

For stable trajectories, the voltages have to be adjusted such that the following equation holds[1]:

$$\beta_x = \sqrt{a_x + \frac{q_x^2}{2}} \in (0, 1) \tag{1.4}$$

Additionally, air friction helps to stabilize the particle tracks since it damps the motion (Stokes' term in the Mathieu equations leads to weaker conditions).

1.1.2 Influence of an Additional Force in z-Direction

Instead of applying an additional potential to both x-plates, it is also possible to apply an additional static electrical field in z-direction (homogeneous, pointing upwards, different potential on the plates). The idea is to compensate the gravitational force which acts on the particle. If considered in the Mathieu equations, a net force in z-direction does not change the shape of the particle tracks but shifts the center of the trajectories. However, if the applied field compensates the gravitational force, there is no shift of the particles and the particle tracks become independent of the applied alternating focusing voltage U_z [1].

1.1.3 Influence of an Additional Alternating Field in x-Direction

As a third option, the influence of an additional alternating field in x-direction is discussed. While the alternating fields U_i have same potential on opposing plates, the field U_W acts homogeneously in x-direction (different potential on opposing plates). The additional term in the Mathieu equation leads to modified trajectories: The particle shakes back and forth. By changing the driving frequency of the field U_W resonances can be observed (forced, damped harmonic oscillator with damping constant k_L from the Stokes' term describing air friction):

$$\omega_W^{res} = \frac{\Omega}{2} \sqrt{\beta_x^2 - 2k_L^2} \tag{1.5}$$

Chapter 2

Experimental Setup

The trap consists basically of 6 copper rings and a high voltage source, see figure 2.1a. The rings are arranged in a cubic geometry: Each two rings facing each other lie on the same potential. The amplitude of the focusing voltages U_x, U_y and U_z can be adjusted individually, but the phase between them remains 120°. Additionally, a lamp and a camera are used to illuminate and observe the trapped particles inside (not visible on the picture). To inject a few particles of aluminum powder, a syringe is installed below the trap. By pressing it, the particles are pushed upwards and become charged by the friction with the surrounding material of the syringe or air.

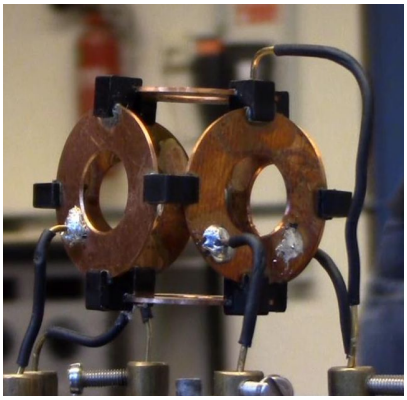

(a) Picture of the Paul Trap during installation. The 6 copper rings are connected to a three phase high voltage supply.

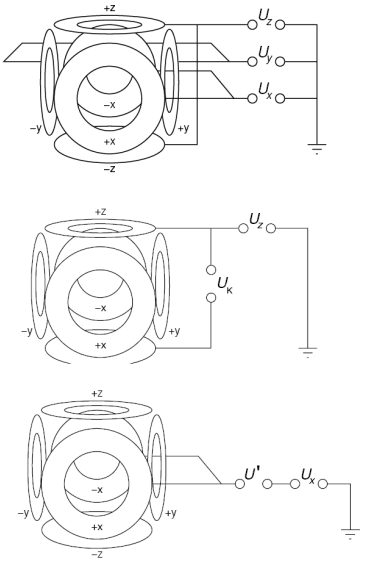

(b) Sketches of the electrical circuits for the additional applied voltages, taken from [1].From top to bottom: The circuits of the alternating fields with phase difference 120°, the constant field in upwards z-direction and the constant potential which can be applied to the x-rings.

Figure 2.1: The experimental setup.

Furthermore, three additional voltages can be applied to some rings of the trap (electrical circuits are shown in figure 2.1b) :

- An additional direct voltage to the two rings in x-direction: U' (same potential on both x-rings)

- A direct voltage between the two z-rings creating a constant electrical field upwards in z-direction (different potential on the two z-rings): U_K
- An overlayed alternating voltage on both x-rings (different potential) creating an alternating field in x-direction: U_W

The second stage of the experimental setup consists of a similar trap and the same electrical circuits, but enclosed in a cylinder. A two-stage vacuum pump is connected to the cylinder and creates a low-pressure environment down to $p \approx 5$ µbar. The vacuum is monitored by a pressure sensor.

Chapter 3

Conduction and Analysis

In the following chapter, the conducted experiments and their results are reported. Each measurement is repeated in the low pressure environment to investigate the influence of air friction on the trapped particles. Since the particle trajectories are much more unstable without air friction, the low pressure cylinder is not evacuated to the lowest limit of the vacuum pump, but operated once at $p = 300\,\text{mbar}$ and once at $p = 180\,\text{mbar}$.

Each conducted measurements yields a value of the specific charge $\frac{q}{m}$ which is different for the aluminum particles because their size and their acquired charge differ. To compare the different methods, the measurements are conducted in a series with the same trapped particle. In the following sections, only those particles are presented where all measurements were successful. The particles trapped in air are called A1, A2, A3 and A4, the ones in vacuum V1 and V2. They are shown in figure 3.1.

As discussed in chapter 4, the output of the high voltage source does not match its adjusted values. The following correction factors are therefore applied to all adjusted voltages and will be justified later:

Voltage	Correction Factor
U_x	0.78 ± 0.02
U_y	0.76 ± 0.03
U_z	0.81 ± 0.03
U_K and U'	0.61 ± 0.01
U_W	0.17 ± 0.03

Table 3.1: Correction factors to compensate for the mismatching output of the voltage source. The determination of these factors is described in chapter 4.

3.1 Measurement I - Stability of the Trajectories

In this measurement, the charge-mass ratio $\frac{q}{m}$ is determined using the stability boundary $\beta = 0$ from equation 1.4.

The electric fields U_i are adjusted to different values between 500 V to 1 000 V, setting the displayed voltages equal on each step $U_x = U_y = U_z$. Starting at $U' = 0$, the additional direct voltage on the rings in x-direction is increased until the observed particle track appears unstable.

Due to the fluctuation of U' and the necessity to keep the particle inside the trap for the two subsequent measurements, the instability criterion has been chosen conservatively:

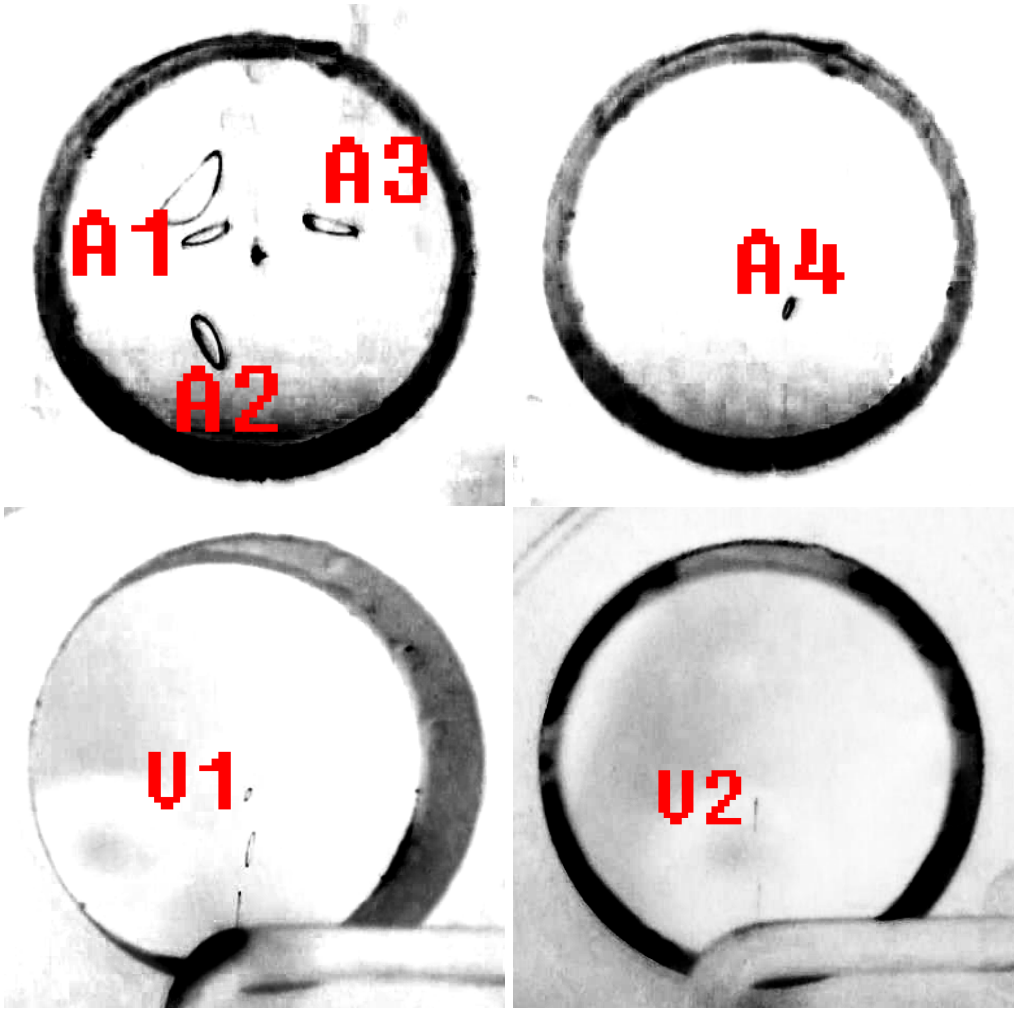

Figure 3.1: Photos of the trapped particles that are analyzed in this work. The images have been cropped and the colors inverted to increase readability.

A track is classified as unstable if any part of the track leaves the observation area visible through the ring facing the camera (figure 3.2).

From the recorded values U_x, U'_{crit} and Ω, the charge-mass ratio can be calculated as follows:

$$\left|\frac{q}{m}\right| = \frac{2}{3} \cdot \frac{r_0^2\,\Omega^2}{K} \cdot \frac{U'_{\text{crit}}}{U_x^2} \tag{3.1}$$

Defining the last term as $a := U'_{\text{crit}}/U_x^2$, the specific charge can be obtained from a linear regression of the recorded values for U' and U_x where the particle became unstable. The assumed errors are discussed in detail in chapter 4, relevant for the linear regression are the statistical uncertainties on U' and U_x, and an uncertainty of 10 % originating from the judgment of instability.

The linear regression is performed as a χ^2-minimization on the function $f(x) = a\,x$. To estimate the parameter error, the linear regression is repeated 1 000 times. Each time, the values for x' and y' are chosen from a normal distribution of width σ_x (σ_y) around x (y). The standard deviation on all fit results is taken as final uncertainty on the parameter a.

The results for the linear regressions are shown in figure 3.3. The first measurement

Figure 3.2: Example for the stability measurement. The highlighted particle track on the upper right side has shifted to the edge of the visible area and is thus classified as unstable. The image has been cropped and the colors inverted to increase readability.

which contains the observation of particles A1, A2 and A3 can only be fitted with a total $\chi^2/\mathrm{ndof} \approx 11$. In this case the linear function does not adequately model the measurement. The fit quality of the other measurements seems better, even though $\chi^2/\mathrm{ndof} < 1$ states that the errors have been overestimated.

For the final q/m value the regression slope is combined with r_0, Ω and K. Using a sliding caliper the width of the trap has been determined to be $2r_0 = (3.050 \pm 0.005)$ cm. The geometry factor K is given in the lab manual as $K = 8$, its uncertainty is assumed to be negligible. $\Omega/2\pi$ is read off the voltage source for each trial run. Its uncertainty is estimated from fluctuations.

Particle	$\Omega/2\pi$ [Hz]	lin. reg. slope [kV^{-1}]	$\lvert\frac{q}{m}\rvert$ [$\mu\mathrm{C\,kg}^{-1}$]	Comment
A1	28 ± 1	0.26 ± 0.02	158 ± 17	low fit quality
A2	28 ± 1	0.24 ± 0.02	143 ± 16	low fit quality
A3	28 ± 1	0.30 ± 0.02	179 ± 19	low fit quality
A4	32 ± 1	0.15 ± 0.02	117 ± 18	
V1	48 ± 1	0.15 ± 0.03	262 ± 46	300 mbar
V2	45 ± 1	0.21 ± 0.04	331 ± 62	180 mbar

Table 3.2: Final results on the charge-mass ratio of the observed aluminum particles, obtained with the stability measurement.

In this and all subsequent calculations, uncertainties are combined using Gaussian error propagation. Table 3.2 shows the final result. All measured particles incidentally have similar charge-mass ratio of $\mathcal{O}\left(100\,\mu\mathrm{C\,kg}^{-1}\right)$.

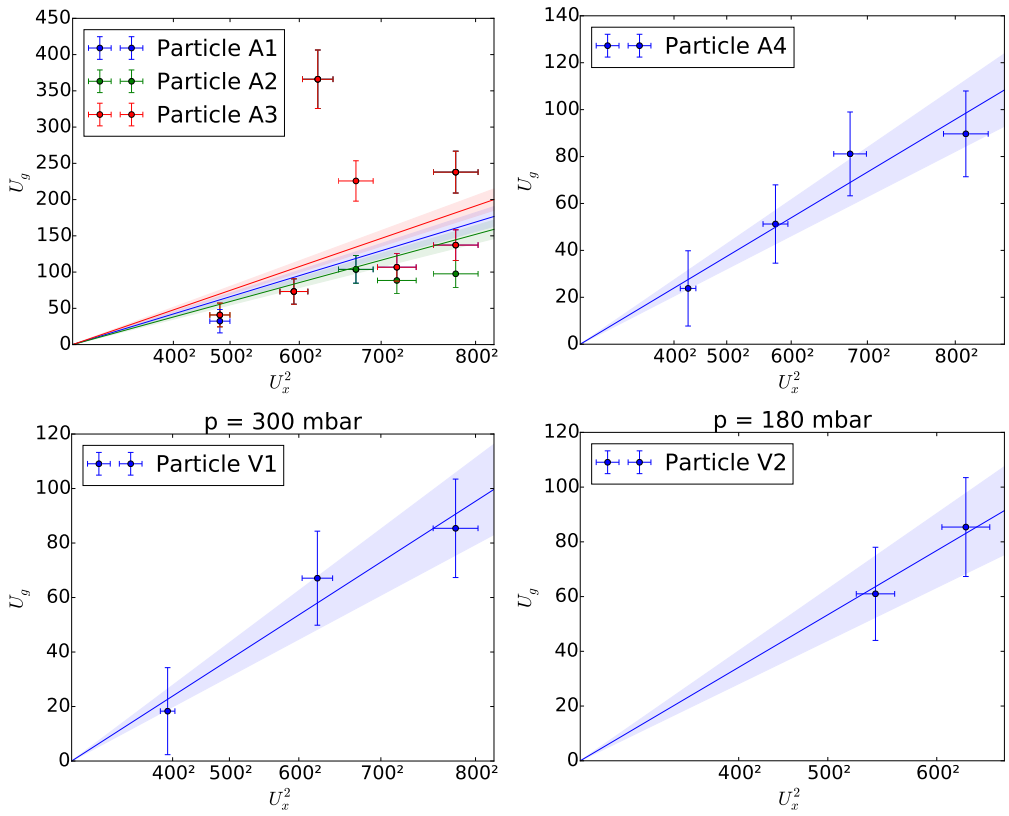

Figure 3.3: Linear regression results. The two upper plots show the results in air, the lower ones in vacuum. The fitted function is shown, with its 1σ confidence band.

3.2 Measurement II - Application of an Additional Field in z-Direction

The second conducted measurement is the compensation of the gravitational force: By increasing the voltage U_K between the two z-rings, a static electric field pointing upwards is created. For each particle with its specific charge, at some point the net force in z-direction becomes zero and the trajectory of the particle becomes independent of U_z. In equilibrium, the following equation must hold and the specific charge can be determined:

$$\vec{F}_G + \vec{F}_{el,z} = 0 \Rightarrow \frac{q}{m} = \frac{g \cdot 2r_0}{U_K} \tag{3.2}$$

For each particle, the recorded and corrected value for U_K is shown in table 3.3 together with the determined specific charge using the gravitational acceleration[2] $g = 9.81\,\mathrm{m/s^2}$ and r_0. The uncertainties on U_K and r_0 are estimated in chapter 4 and propagated here.

Particle	$U_K^{\text{compensate}}$ [V]	$\frac{q}{m}$ [mC kg^{-1}]
A1	26 ± 15	12 ± 7
A2	26 ± 15	12 ± 7
V1	43 ± 15	7 ± 3
V2	40 ± 15	8 ± 3

Table 3.3: Results from the z-compensation measurement: U_K and the resulting specific charge.

3.3 Measurement III - Resonance Study

In this last measurement, an additional alternating voltage is applied between the two rings in x-direction. The frequency ω is adjusted independently of Ω, between 6 Hz to 50 Hz.

By observing the oscillations on the camera image, the resonance frequency ω_{res} is obtained, manifesting itself as Lissajous figure.

The mass-charge ratio q/m is then calculated from equation 1.5, setting $k_L = 0$ and using $U' = 0$ ($a_x = 0$):

$$\frac{q}{m} = \frac{\Omega r_0^2}{\sqrt{2} K U_x} \omega_{\text{res}} \tag{3.3}$$

Particle	U_x [V]	$\Omega/2\pi$ [Hz]	$\omega_{\text{res}}/2\pi$ [Hz]	$\frac{q}{m}$ [µC kg^{-1}]	Comment
A1, A2, A3	484 ± 17	28 ± 1	14 ± 1	657 ± 61	indistinguishable
A4	640 ± 20	31 ± 1	16 ± 1	610 ± 52	
V1	764 ± 22	28 ± 1	14 ± 1	416 ± 38	300 mbar
V2	546 ± 18	44 ± 1	22 ± 1	$1\,439 \pm 99$	180 mbar

Table 3.4: Results from the resonance study. One can see that the resonances occur at about half the focusing frequency. In case of A1, A2 and A3, the resonance seems to happen at the same frequency.

Here the air friction has been neglected. Because no amplitude difference is visible on the resonances (see table 3.5), obtaining the air friction coefficient is impossible from this measurement.

Due to the observation of all resonance very close to half of the respective focusing frequencies, it seems that the outcome of this measurement does not primarily depend on q/m, but that the Lissajous figures appear exactly at $\Omega/2$. Consequently, it would be only a coincidence that the obtained charge-mass ratio has the right order of magnitude.

$\omega/2\pi$ [Hz]	Amplitude on screen [mm]	Comment
6	5	
10	3	
15	3.5	Lissajous figure observed
21	3.5	
24	3	
31	3	Beat
39	2.5	
51	3	

Table 3.5: Example resonance measurement for particle V1 at $\Omega = 28\,\text{Hz}$. The frequency ω is varied and the oscillation is read off the computer screen in mm.

Chapter 4

Uncertainties

4.1 High Voltage Source

4.1.1 Mismatch of the Internal Voltage Measurement

The high voltage source displays the adjusted voltage. However, a cross-check measurement with a multimeter shows discrepancies for all voltages of the source. To account for this, correction factors have been introduced in chapter 3. They were determined by adjusting four different voltages, measuring them with the multimeter and comparing them to the displayed values. The ratio of the measured and adjusted values is averaged and the standard deviation is computed. The results are shown in table 3.1 and are used in the analysis as correction factors. The systematic uncertainty which arises from the uncertainty on these correction factors is negligible compared to other uncertainties which are discussed in the following.

4.1.2 Fluctuations of the Voltage Source

The displayed voltage values on the voltage source fluctuate strongly. To read-off a voltage value, approximately four subsequent values are averaged live during the adjustment. The uncertainties arising from this can be estimated as follows: A longer set of voltage values is recorded ($N \approx 20$), subsampled in sets of four and the mean of each set is determined. The standard deviation of the mean values obtained this way is calculated. It is used as an estimator for the fluctuation. The subsampling simulates the read-off process and yields the following uncertainties on the voltage values:

Voltage	Uncertainty [V]
U_x	11
U_y	12
U_z	6
U_K and U'	16
U_W	8

Table 4.1: Uncertainties on the adjusted voltage values arising from the fluctuating display of the voltage source.

4.2 Evaluation of the Track Stability

During measurement II, the constant voltage U' is increased until the particle trajectory becomes instable. However, the point of instability can be determined only to a precision of roughly 10 %: The trajectory could as well be called instable if U' is increased or decreased in this range.

4.3 Frequency of the Alternating Fields

The frequency of the alternating fields which is displayed on the voltage source can not be cross-checked in this setup. However, there is still a fluctuation which can be taken into account: The adjusted frequency is instable in the range of ± 1 Hz. This uncertainty is treated in all analysis steps as statistical error.

4.4 Distance Measurements

The distance r_0 from the rings to the center of the trap is used in all analysis steps. It is determined with a sliding caliper between opposing rings. The uncertainty (difference between r_0 in x,y or z-direction) is estimated to $\sigma_{r_0} \approx 0.25$ mm. The influence of this uncertainty is negligible compared to other discussed uncertainties. The same holds for the measurements of the ring diameter which is used to find the scale for the oscillation amplitude in measurement III.

Chapter 5

Conclusion

5.1 Methods and Results

In this report, three measurements of the specific charge of aluminum particles in a Paul Trap are presented. The results are plotted in figure 5.1 and show strong discrepancies. Therefore, averaging the result from different methods for one particle is not possible.

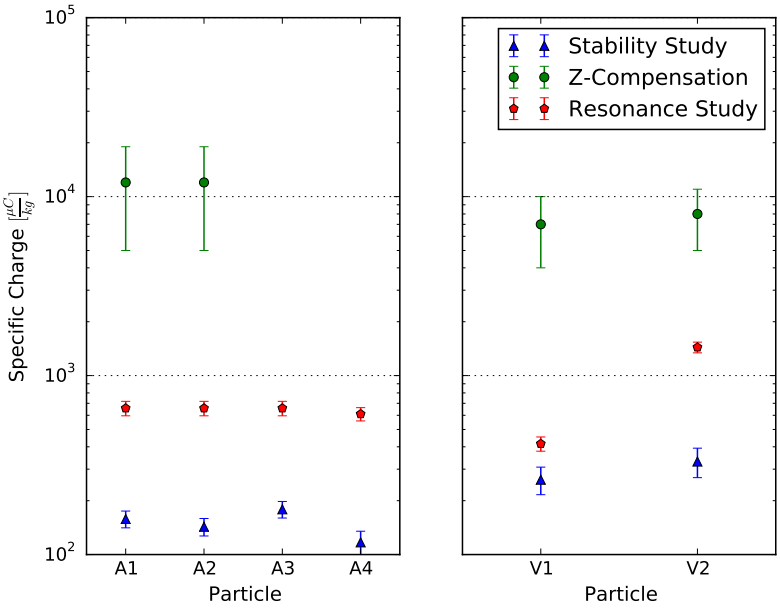

Figure 5.1: Overview of the measured specific charge. Comparison between different measurement methods for each particle.

Since none of the methods is intrinsically better than the others, this report cannot state one single answer about the charge-mass ratio. One can only state that the measurement III (resonance study) under the influence of an additional alternating field does not seem very trustworthy.

5.2 Outlook

The entire experiment could yield much better results if a more accurate voltage source would be provided, which delivers more stable voltages and finer tuning of the frequencies.

One notable subsequent calculation that can be done from this report's results is the determination of the particles absolute charge. The manufacturer of the aluminum powder states a diameter of $d = 30\,\mu\text{m}$. Assuming spherical particles and the density of aluminum $\rho = 2.7\,\text{g}\,\text{cm}^{-3}$, the charge can be calculated as

$$Q = \frac{q}{m} \cdot \rho \cdot \frac{4\pi}{3} \left(\frac{d}{2}\right)^3 \tag{5.1}$$

The results are shown in table 5.1. The number of electrons might seem large, but compared to Avogadros number $\approx 10^2 3$, the result sounds reasonable.

Method	q/m [$\mu\text{C}\,\text{kg}^{-1}$]	Q
Stability	$\mathcal{O}\left(10^2\right)$	$\mathcal{O}\left(10^{10}e\right)$
z-Compensation	$\mathcal{O}\left(10^4\right)$	$\mathcal{O}\left(10^{12}e\right)$
Resonance	$\mathcal{O}\left(10^3\right)$	$\mathcal{O}\left(10^{11}e\right)$

Table 5.1: Estimation of the total charge of each particle. Divided by the elementary charge, this yields the number of electrons which have been transfered.

Bibliography

[1] RWTH-Aachen, "Experiment XIII The Paul Trap Laboratory class particle physics," 2013.

[2] F. a. Bundesamt für Kartographie und Geodaesie (BKG), "Die gravimetrischen Messverfahren," 2013. http://www.giz.wettzell.de/Vortraege/Gravimetrie/Wettzell_Gravimetrie10_06.pdf.